

Effect of Ca content on the conduction mechanism for $\text{Ni}_{0.7-x}\text{Zn}_{0.3}\text{Ca}_x\text{Fe}_2\text{O}_4$ nanocomposites at $0.2 \leq x \leq 0.7$

Mahmoud Hosseney Makled

Faculty of science, Physics department, Benha University, 13518 Benha, Egypt.

Abstract: $\text{Ni}_{0.7-x}\text{Zn}_{0.3}\text{Ca}_x\text{Fe}_2\text{O}_4$ nanoparticles with different Ca concentration were synthesized by chemical coprecipitation technique at different annealing temperatures. The influence of Ca content on the electrical conduction was investigated as a function of frequency and temperature. The ac conductivity, σ_{ac} , was found to be increases with both temperature and frequency, confirmed semiconductor behavior for all samples. The addition of Ca^{2+} decrease σ_{ac} up to certain Ca content. The calculated values of activation energies mainly increase with Zn^{2+} content and sintering temperature. The dependence of σ_{ac} on frequency is governed by the relation $\sigma_{ac} = A\omega^s$. The calculated values of s recorded decreasing with increasing temperature for all studied samples. In the low temperature range, the values of s obeying the polaron hopping conduction mechanism. Whereas at high temperature, the values of s lie between 0.5 to about 0.1 confirming the ionic diffusion of Ni ions. The dielectric constant ϵ' was measured for all samples and found to be obeying Debye dispersion relation in wide range of frequencies and temperatures.

Keywords- Conduction mechanisms, Nanocomposites, Dielectric, coprecipitation

Date of Submission: 16-05-2020

Date of Acceptance: 31-03-2020

I. Introduction

The most important characteristics of soft ferrites are their high permeability, high electrical resistivity and low losses [1,2]. Nickel and substituted nickel ferrite consider as one of the most important technological materials due to the high electrical resistivity coupled with low magnetic losses. The high frequency applications in the field of telecommunication need some ferrite with excellent electrical and magnetic properties [3,4]. In general, the electrical properties of ferrites depend on the cation distribution in both tetrahedral (A-site) and octahedral (B-site) [5,6]. On the other hand, the spinel ferrites can be used only up to 3 GHz frequency range, due to their crystal structure limits cut-off frequency. But the hexaferrite, as strontium and barium ferrites can be used in the whole GHz region, due to their intrinsic uni-axial anisotropic property [7–10]. Ca has the same electronic configuration as Sr and Ba, but there are no studies available concerning Ca doped NiZn ferrite nanoparticles. On the other hand, Ca belongs to the types of additives that segregate to the grain boundaries and affect the grain boundary resistivity, whereas, the other additives can affect microstructure [11–13]. So, in the present study, Ca^{2+} ion was chosen to clarify its effect on the electrical properties of NiZn ferrite.

Synthesis, characterization and magnetic properties of nanocrystalline $\text{Ni}_{1-x}\text{Zn}_x\text{Fe}_2\text{O}_4$ and $\text{Ni}_{0.7-x}\text{Zn}_{0.3}\text{Ca}_x\text{Fe}_2\text{O}_4$ spinels are achieved in previous work in details [14, 15]. The present work will focus on the conduction mechanism of $\text{Ni}_{0.7-x}\text{Zn}_{0.3}\text{Ca}_x\text{Fe}_2\text{O}_4$ ferrite with $0.2 \leq x \leq 0.7$.

II. Experimental details

2.1 Ferrite preparation

Ferrite nanoparticles $\text{Ni}_{0.7-x}\text{Zn}_{0.3}\text{Ca}_x\text{Fe}_2\text{O}_4$ ($0.0 \leq x \leq 0.7$) were prepared by the chemical coprecipitation route. The final sintering was done at 600 and 1000 °C with subsequent slow cooling to room temperature. The as-dried and sintered ferrites were characterized using an X-ray, scanning electron microscope, Atomic force microscopy, thermal analysis and IR characterization in addition to the magnetic properties. The details of the method of preparation and characterization have been given in an earlier publication [15].

2.2 Electrical measurements

The ac electrical conductivity and dielectric properties for the investigated samples were performed over a temperature range from room temperature up to 700 K at different frequencies ranging from (100kHz → 5MHz) using LCR Hi Tester (HIOKI model 3531Z Japan).

Samples in the disc form of about 0.85 cm diameter and 0.16 cm thick are used. The two surfaces of each sample are will polished, coated with silver paint and checked for good conduction.

III. Results and discussion

3.1 Frequency dependence of ac conductivity

The variations of the ac conductivity, σ_{ac} , with frequency for investigated samples of $Ni_{0.7-x}Zn_{0.3}Ca_xFe_2O_4$ ferrite nanoparticles with $(0.2 \leq x \leq 0.7)$ calcined at 600 °C and 1000 °C, is shown in fig.1. From this figure, it is noticed that σ_{ac} remains almost constant in a relatively low frequency region then it increases in the higher frequency region. The results could be explained in terms of two regions depending on the applied frequency; region I (100 kHz- 400 kHz) and region II (400 kHz- 5 MHz). This type of behavior shows that more than one activation barriers with different activation energies exist in these samples. The frequency dependent ac conductivity curve at low frequency is attributed to the decrease in the hopping frequency. This is due to a reduction in the mobility of the charge carriers resulting in an increase in the grain boundary resistance. This decreases the probability of charged carriers crossing over the grain boundary.

Generally, the increasing in ac conductivity with the applied frequency in such ferrites can be explained on basis that the pumping force of the applied frequency that helps in transforming the charge carriers between the different localized states as well as liberating the trapped charges from the different trapping centers. These charge carriers participate in the conduction process simultaneously with electrons produced from the valence exchange between the different metal ions [16]. In other words, increases in frequency enhance the electron hopping between Fe^{3+} and Fe^{2+} sites. Hole hopping between Ni^{2+} and Ni^{3+} at B-site also contribute to electric conduction in ferrites. The ac electrical frequency dependence can be explained with the help of Maxwell-Wagner two-layer models or heterogeneous model of the polycrystalline structure of ferrites [17]. In region I the conduction is due to the resistive grain boundaries. Also, the grain boundaries are more active and the electron hopping probability between $Fe^{2+} \leftrightarrow Fe^{3+}$ ions or hole hopping probability between $Ni^{3+} \leftrightarrow Ni^{2+}$ ions nearly negligible. In region II the dependence of ac conductivity on frequency can be expressed according to the general equation;

$$\sigma_{ac} = A \omega^s$$

Where σ_{ac} , is the alternating current conductivity, A is the temperature dependent constant, ω is the measuring frequency and the frequency exponent $s \leq 1$.

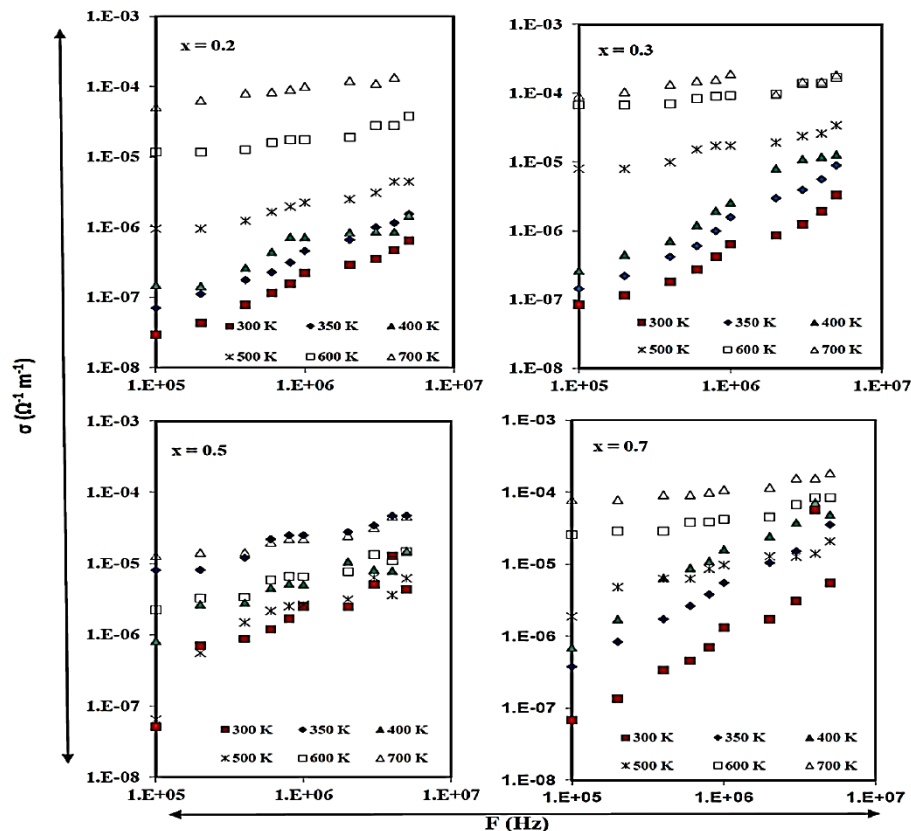


Fig. 1a. Frequency dependence of ac conductivity for $Ni_{0.7-x}Zn_{0.3}Ca_xFe_2O_4$, $(0.2 \leq x \leq 0.7)$ calcined at 600 °C

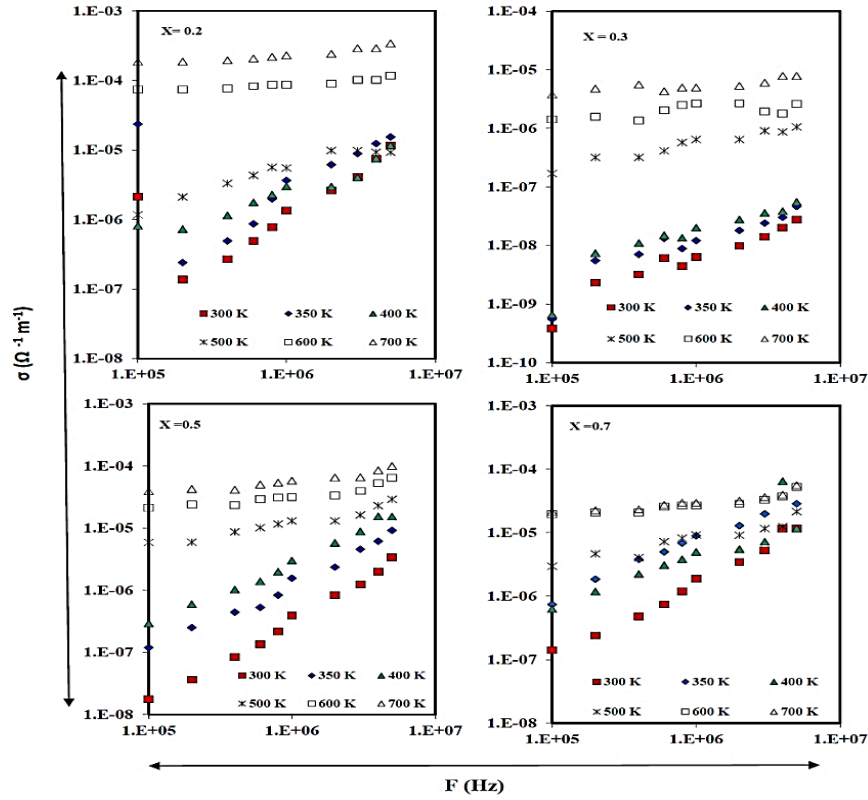


Fig. 1b. frequency dependence of ac conductivity for $Ni_{0.7-x}Zn_{0.3}Ca_xFe_2O_4$, ($0.2 \leq x \leq 0.7$) calcined at $1000\text{ }^\circ\text{C}$

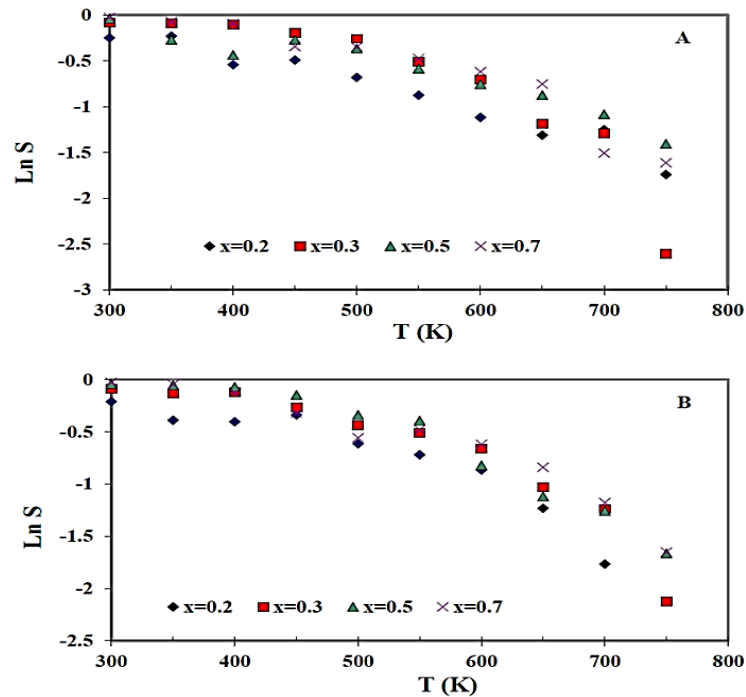


Fig. 2. The variation of the exponent (s) with temperature (a) at $600\text{ }^\circ\text{C}$ (b) at $1000\text{ }^\circ\text{C}$ for $Ni_{0.7-x}Zn_{0.3}Ca_xFe_2O_4$, ($0.2 \leq x \leq 0.7$).

The values of 's' have been calculated from previous figures at different temperatures and redrawing in fig. 2 against temperatures. To clarify the dependence of conduction mechanisms on the exponent s, fig. 2 illustrates the variation of $\ln s$ with temperature for NiZnCa ferrite calcined at 600 and 1000 °C. From the figures, it is noticed that two regions in $\ln s$ -T relation appear, the first is related to low temperature range while the second appear in the high temperature range.

At relatively low temperature $T < 550K$, the values of s decrease slowly ($0.5 \leq s \leq 1$) and follow a linear variation. In this temperature range, the conduction is electronic while at relatively high temperature $T > 550 K$, the exponent s decrease rapidly ($0 \leq s \leq 0.5$) and the conduction is ionic. The conductivity increases by increasing the temperature due to the increase in the lattice vibration which leads to increase in charge carriers. Then the ions become very close to each other with high probability for charge transfer to occur. Therefore, from the trend of the variation of s with temperature, it may be concluded that the ac conductivity in the Ni-Zn-Ca ferrite samples may be described by the CBH model. In general NiZnCananoferrite structures accommodate oxygen interstitial, at which a charge compensated by holes, to exhibit p-type conduction according to: $\frac{1}{2} O_{(g)}^2 \leftrightarrow O''_i + 2 h'$, where in iron-containing compounds, the holes may be associated with Fe^{3+} cations, forming small polaron, to essentially produce a fraction of Fe^{4+} cations as: $Fe^{3+} + h' \rightarrow Fe^{4+}$. Therefore, the fraction of Fe^{4+} , directly related to the concentration of charge carriers. This conduction mechanism is consistent with charge transport by holes, which hop between Fe^{3+} ions thereby introducing a fraction of Fe^{4+} ions during the association of the hole with an iron cation. However, as Ca^{2+} content increases up to $x=0.3$, large concentration of holes created by Ca^{2+} or Ni^{2+} ions lead to a decrease in their mobility, hence the decrease in conduction. In ferrites with $x > 0.3$, large concentration of Ca^{2+} induces large amounts of Fe^{4+} on the expense of Fe^{2+} existed at B-site.

3.2 The dependence of electrical conductivity on the Ca content

Fig. 3a illustrates the ac conductivity (σ_{ac}) dependence on Ca content for $Ni_{0.7-x}Zn_{0.3}Ca_xFe_2O_4$ ferrite ($0.2 \leq x \leq 0.7$) calcined at 600 °C and 1000 °C. From this figure it is noticed that, the addition of Ca^{2+} ions decrease the electrical conductivity of NiZnCananoferrite.

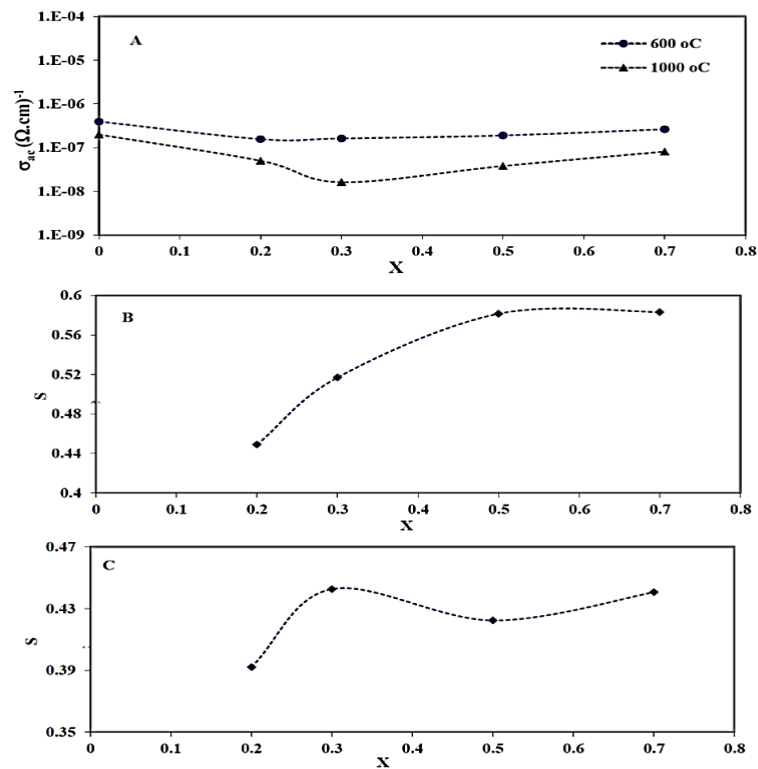


Fig. 3. The dependence of (a) ac conductivity (b) average (s) at 600 °C (c) average (s) at 1000 °C on Ca content for $Ni_{0.7-x}Zn_{0.3}Ca_xFe_2O_4$ ($0.0 \leq x \leq 1.0$).

From previous work, we can see, increasing Ca content decreasing grain size and increasing porosity [15]. Decreasing the grain size, increasing grain boundary resistivity and increasing activation energy reduce eddy current. The electrical conductivity of the polycrystalline ferrite can be decreased by increasing grain boundary resistivity and reducing grain size according to the general relation ($R_{\text{bulk}}=R_{\text{g,b}}+R_{\text{g}}$) [16]. The multivalent nature of iron and nickel allow the occurrence of conduction through holes or electrons hopping process. The non-multivalent nature of zinc and calcium can reduce the electron/hole hopping in such materials. From XRD, SEM studies the grain size for all samples decreases as Ca²⁺ content increases due to hindrance of grain boundary mobility. Accumulation of Ca²⁺ at the grain boundaries leading to grain boundary thickening showing increase in resistivity. IR spectra show that ν_2 -band splitted and broadened suggesting vacancies on B-site. Meanwhile Ca²⁺ increases the porosity of ferrite which in turns increases the resistivity.

Vacancies, holes created by Ca²⁺ and porosity, all leading to enhanced resistivity for the material. The composition dependence of conductivity σ_{ac} reveals that cation distribution has a prime role in conduction. In ferrites calcined at 600 °C, Ca²⁺ ions occupy A-site in all samples as reveals from XRD and IR spectra. This leads to the migration of equivalent number of Fe³⁺ ions from A to B-site, which results in Fe³⁺ increases at B-site, consequent Fe²⁺/Fe³⁺ ratio slightly increases and hence the σ_{ac} . This is shown when $x>0.3$, but in ferrites with Ca content $x\leq 0.3$, the presence of higher Ni²⁺ content, i.e., Ni³⁺-Ni²⁺ hole concentration, in addition to Fe²⁺-Fe³⁺ electron conduction, compensates each other, and drift mobility decreases and hence σ_{ac} slightly decreases.

On the other hand, when the ferrite calcined at 1000 °C, its behavior is intrinsic, i.e., depends only on the composition but not on grain size or other surface impurities. The decrease in ac conductivity by increasing the calcination temperature from 600 to 1000 °C, indicates the removal of surface defective layer before 1000 °C (≈ 700 -750 °C) as confirmed from DSC analysis which control the behavior of ferrites at 600 °C. From IR and XRD studies, Ca²⁺ ions occupy B-site in ferrites calcined at 1000°C with $x\leq 0.3$, therefore the bigger Ca²⁺ ion increase the interatomic distance between Ni³⁺-Ni²⁺ and Fe²⁺-Fe³⁺, resulting in an increase in resistivity. Ferrite with composition Ni_{0.4}Zn_{0.3}Ca_{0.3}Fe₂O₄ has the highest resistivity among all the series. When Ca²⁺ content increases when $x>0.3$, Ca²⁺ ions occupy A-site, therefore high Fe³⁺ concentration at B-site increases the Fe²⁺-Fe³⁺ electron exchange at B-site, which is the main conduction mechanism in ferrites, as depicted in ferrite with $x=0.7$.

Fig.3b illustrates the dependence of the Ca²⁺ content on the average values of the exponent s for Ni_{0.7-x}Zn_{0.3}Ca_xFe₂O₄ ferrite ($0.2\leq x\leq 0.7$) calcined at 600 °C and 1000 °C respectively. From the figures, there is a continuous increase of s with increasing Ca content. This increase in s values with increasing Ca content may be due to that the replacement of Ni ion (0.67 Å) by Ca ion (0.99 Å) reduce the charge hopping inside the ferrite leading to the increase in s values. Also, as Ca content increases, the resistivity increases due to the accumulation of Ca²⁺ at the large grain boundaries leading to grain boundary thickening. Due to the larger radius of Ca with respect to Ni²⁺, Zn²⁺ or Fe³⁺, some of Ca²⁺ ions fail to enter the ferrite lattice and accumulate at the grain boundaries. This results in stresses in the ferrite which increase as Ca ion content increases. From Fig. 3, it is observed that the value of s has the maximum value for Ni_{0.4}Zn_{0.3}Ca_{0.3}Fe₂O₄ ferrite sample at calcination temperature 1000 °C. The increase in s at this value of x (0.3) may be due to the cation redistribution of Ca²⁺ in this ferrite. From XRD and IR data, it is observed that Ca²⁺ ions recite at B site at $x\leq 0.3$ and at A site in ferrite with $x>0.3$. The presence of big size Ca²⁺ ions between Fe³⁺ ions at B site decrease the drift mobility. Also, at this concentration of Ca ($x\leq 0.3$) the presence of Ca²⁺ in B-site affect the distant between Ni³⁺-Ni²⁺ which results in the observed increase in s values.

3.3 Dielectric studies

Fig.4 shows the frequency dependence of the dielectric constant (ϵ) at different temperatures for Ni_{0.7-x}Zn_{0.3}Ca_xFe₂O₄ ($0.2\leq x\leq 0.7$) samples calcined at 600 and 1000 °C. From this figure one can noticed that, ϵ decreases with increasing frequency. The dispersion is rapid at lower frequency range (10^5 - 10^6 Hz) which is due to interfacial polarization. At higher frequency range, due to rotational displacements of the dipoles which results in the orientational polarization, dispersion in dielectric constant becomes small approaches a near frequency independent response [18]. This is a normal trend in such materials because the species contributing to the polarizability are lagging the applied field at higher frequency. This type of dielectric behavior in the ferrites has been explained by the Maxwell-Wagner and Koop's phenomenological theory [19]. In these models, a dielectric medium is assumed to be made up of highly conductive grains and poorly conducting grain boundaries. The grain boundaries are more effective at lower frequencies while the grains are found to be more effective at higher frequencies. The large values of the dielectric parameters at lower frequency are mainly due to the presence of all type of polarization. According to Sarah and Suryanarayana [20]. The polarization in ferrites occurs through a mechanism like the conduction process. The exchange of electrons between ferrous

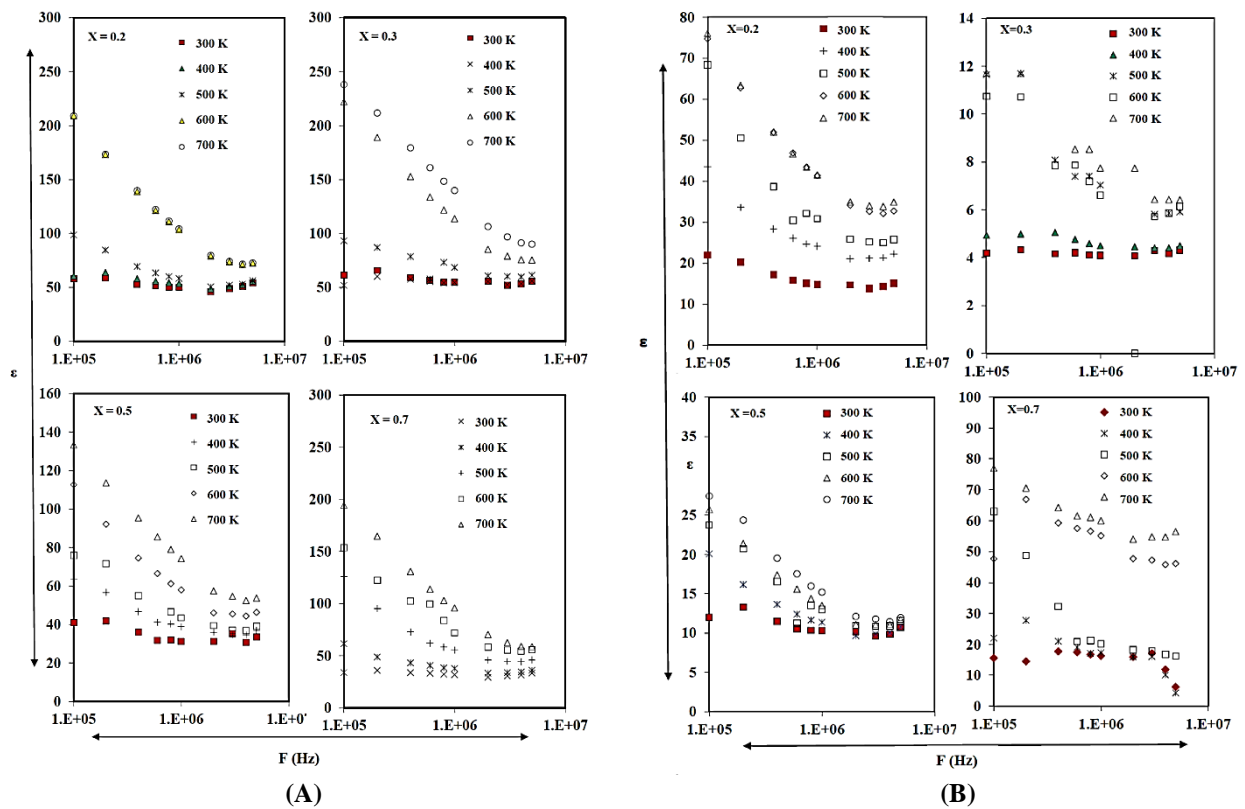


Fig. 4. Frequency dependence of real part of dielectric constant (ϵ) for $Ni_{0.7-x}Zn_{0.3}Ca_xFe_2O_4$, ($0.2 \leq x \leq 0.7$) calcined at a, 600 and b, 1000°C.

ions (Fe^{2+}) and ferric ions (Fe^{3+}) on octahedral site may led to local displacement of electrons in the direction of applied field and these electrons determine the polarization. The electrons must pass through the well-conducting grains and the poorly conducting grain boundaries. As the grain boundaries have large resistance, the electrons pile up there and produce large space charge polarization.

Fig.5 illustrates the variation in dielectric constant of NiZnCa ferrites of different Ca compositions, sintered at various sintering temperatures. From this figure the values of ϵ decrease with increasing Ca^{2+} content calcined at 600 °C. For samples calcined at 1000 °C, the dielectric constant decreases with the increase of Ca^{2+} content up to $x=0.3$, after which ϵ start to increase with further increase of Ca^{2+} content up to $x=0.7$. For samples calcined at 600 °C, Ca^{2+} occupy A-site, so the concentration of Fe^{3+} at B-site increases, hence Fe^{4+} . Further increase in Ca^{2+} content increases the Fe^{4+} on the expense of Fe^{2+} , which increases the concentration of $Fe^{3+}-Fe^{4+}$ pairs on B-site. When the calcination temperature increases to 1000 °C, removal of surface layer occurs, meanwhile cation redistribution takes place. Therefore, at this calcination temperature, the dielectric constant (ϵ) decreases with the increase of Ca^{2+} content up to $x=0.3$, after which ϵ start to increase with further increase of Ca^{2+} content up to $x=0.7$. For ferrites with Ca^{2+} content $x=0.2$ and $x=0.3$, Ca^{2+} ions occupy B-site, whereas for ferrite with $x>0.3$, it occupies mainly A-site. In ferrites with $x=0.2$ and $x=0.3$ the presence of Ca^{2+} at B-site, increases the distance between $Fe^{2+}-Fe^{3+}$ ions, hence the rate of $Fe^{2+}-Fe^{3+}$ electron exchange decreases. In addition, the increase in Fe^{4+} holes number which results from number of holes (Fe^{4+}), the addition of Ca^{2+} decreases Fe^{2+} concentration and hence ϵ' , ϵ'' and $\tan\delta$ decrease. Whereas the increase in ϵ for samples with $x>0.3$, is due to the migration of some Fe^{3+} from A- to B-site as a result of occupying Ca^{2+} A-site, which in turn increasing the conduction and ϵ . The increased thickness of grain boundaries as a result of segregation Ca^{2+} ion at grain boundaries, in addition to stresses, increases the resistivity of the ferrites.

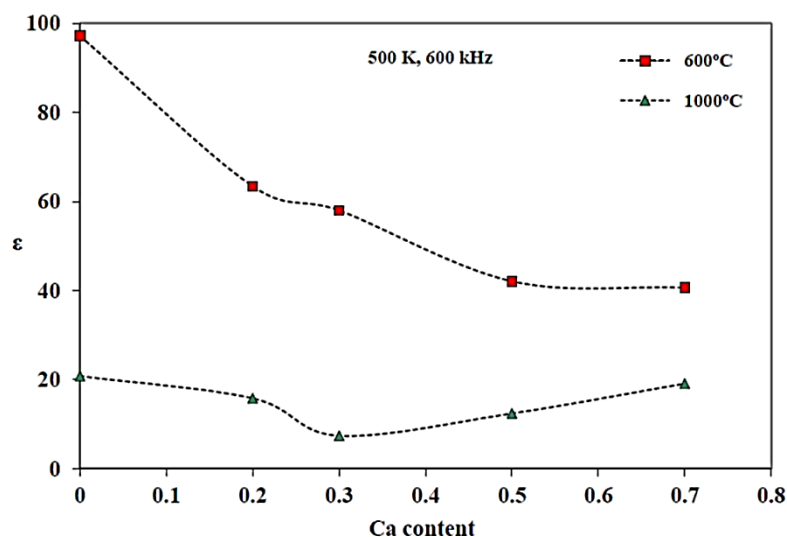


Fig. 5. Dielectric constant dependence on Ca content for samples at constant temperature and frequency for $Ni_{0.7-x}Zn_{0.3}Ca_xFe_2O_4$ ($0.2 \leq x \leq 0.7$) calcined at 600 and 1000 °C.

IV. Conclusion

Nanocrystalline composition $Ni_{0.7-x}Zn_{0.3}Ca_xFe_2O_4$ ($0.0 \leq x \leq 0.7$) ferrites calcined at 600 °C and 1000 °C are successfully synthesized using coprecipitation wet method. The obtained ferrite illustrates semiconductor behavior with conductivity in the range (10^{-6} - $10^{-8} \Omega^{-1}cm^{-1}$). At lower temperature $T < 550K$, the calculated values of σ mild decrease with increasing temperature, however, for $T > 550K$ it decreases rapidly with the increasing temperature reflects the CBH of conduction.

The σ_{ac} decrease with Ca^{2+} content and decrease with increasing calcination temperature. The decreasing in dielectric constant was explained according to highly conductive grains and poorly conducting grain boundaries.

The dielectric constant is highly influenced by Ca content and annealing temperature, due to the migration and concentration of Ca, Ni, and Fe ions in tetra and octahedral sites

References

- [1]. H. Shokrollahi, K. Janghorban, J. Magn. Magn. Mater. **308**, 238 (2007)
- [2]. H. Shokrollahi, K. Janghorban, Iran. J. Sci. Technol. Trans. B: Eng. **30**, 413 (2006)
- [3]. J. Azadmanjiri, H.K. Salehani, M.R. Barati, F. Farazan, Mater. Lett. **61**, 84 (2007)
- [4]. Z. Yue, L. Li, J. Zhou, H. Zhang, Z. Gui, Mater. Sci. Eng. B **64**, 68 (1999)
- [5]. U.N. Trivedi, K.H. Jani, K.B. Modi, H.H. Joshi, Mater. Sci. Lett. **19**, 1271 (2000)
- [6]. X. Fua, H. Geb, Q. Xinga, Z. Pengb, Mater. Sci. Eng. B **176**, 926 (2011)
- [7]. M.J. Iqbal, M.N. Ashiq, I.H. Gul, J. Magn. Magn. Mater. **322**, 1720 (2010)
- [8]. Y. Bai, J. Zhou, Z. Gui, L. Li, J. Magn. Magn. Mater. **246**, 140 (2002)
- [9]. R.S. Meena, S. Bhattacharya, R. Chatterjee, J. Magn. Magn. Mater. **322**, 2908 (2010)
- [10]. S.M. Abbas, A.K. Dixit, R. Chatterjee, T.C. Goel, J. Magn. Magn. Mater. **309**, 20 (2007)
- [11]. K.V. Kumer, D. Ravinder, Mater. Lett. **52**, 166 (2002)
- [12]. O. Caltun, L. Spinu, A. Stancu, J. Optoelectron. Adv. Mater. **2**, 337 (2002)
- [13]. C.R. Hendricks, V.W. Amarakoon, D. Sullivan, Ceram. Bull. **5**, 817 (1991)
- [14]. M. H. Maklad, N. M. Shash, H. K. Abdelsalam, Inter. J. Modern Phy. B **28**, 1450165-1 (2014)
- [15]. M. H. Maklad, N. M. Shash, H. K. Abdelsalam, Europ. Phy. J. Appl. Phy. **66**, 30402 (2014)
- [16]. N. Jaiswal, D. kumar, S. Upadhyay, O. Parkash, J. Alloys & Comp. **577**, 456 (2013)
- [17]. J. Ding, Y. J. Chen, Y. Shi, S. Wang, Appl. Phy. Lett., **77**, 3621 (2000)
- [18]. N. Ponpandian, A. Narayanasamy, J. Appl. Phy. **92**, 2770 (2002)
- [19]. C. G. Koop, Phy. Rev. **83**, 121 (1951)
- [20]. P. Sarah, S. V. Suryanarayana, Indian J. Phy. **77**, 449 (2003)